

**APPLICATION OF VISCO-ELASTIC MODELS TO FLEXIBLE PAVEMENT ANALYSIS**

Author names: **J W Maina<sup>1</sup>, J Anochie-Boateng<sup>1</sup>, K Matsui<sup>2</sup>**

1: CSIR Built Environment  
P O Box 395  
Pretoria, 0001

2: Dept. of Civil and Environmental Engineering  
College of Science and Engineering  
Tokyo Denki University  
Ishizaka, Hatoyama, Hiki, Saitama,  
350-0394 Japan

**Abstract**

A revision of the South African mechanistic-empirical pavement design method (SAPDM) is ongoing. The SAPDM will use dynamic modulus ( $|E^*|$ ) as the modulus of hot-mix asphalt (HMA) materials. The  $|E^*|$  is required in order to compute stresses, strains and displacements in flexible pavements. In this regard,  $|E^*|$  will typically be used as a modulus parameter indicative of linear viscoelastic (LVE) behaviour of HMA materials at different temperatures and load frequencies. In the process of carrying out the work, it has become clear that there are areas, not considered at the inception of the SAPDM project, that require further research and development because of their potential for significant impact to the industry. One such area is on the type of information that may be obtained from the ongoing laboratory testing of dynamic (complex) modulus of hot-mix asphalt (HMA) and how that information can be utilized in the mechanistic analysis of pavement structures.

In preparation for future update of SAPDM, this paper demonstrates the use of rheological models to characterize LVE behaviour of HMA material at different temperatures and loading frequencies. Further, the paper presents some mathematical formulation that may be used to analyze a pavement system consisting of one or more layers of LVE materials. Two rheological models mentioned in the literature as already verified for flexible pavement application i.e. Burger's and Huet-Sayegh models are implemented and incorporated into the analysis algorithm.

In conclusion, determination of parameters for both Burger's and Huet-Sayegh models was successful. Further, the two models have been incorporated into a multilayer linear viscoelastic (MLLVE) algorithm and pavement surface deflections are used to compare the two models where Huet-Sayegh model resulted in lower responses compared to Burger's model. Future research will focus on validation of the algorithms and also the development of a protocol for the determination of rheological model parameters.

## 1. INTRODUCTION

The South African National Road Agency Limited (SANRAL), in partnership with the CSIR, is funding revision and improvement of the South African Pavement Design Method (SAPDM) for flexible road pavements. This will be an improvement on the current South African Mechanistic Design Method (SAMDM) as described by Theyse *et al.* (1996). One of the sub-projects entails laboratory testing of hot-mix asphalt (HMA) samples to obtain the modulus of the material. The complex moduli (dynamic moduli and phase angles) are obtained at a number of temperature and frequency combinations under sinusoidal loading conditions. The complex modulus ( $E^*$ ) is a viscoelastic response and it contains both real and imaginary components. By definition from linear viscoelastic (LVE) theory, the absolute value of the complex modulus is the dynamic modulus  $|E^*|$  although dynamic modulus is generally related to modulus that has been determined under dynamic load condition. The SAPDM will use dynamic modulus to characterize the elastic modulus of HMA materials. The  $|E^*|$  is required in order to compute stresses, strains and displacements in flexible pavements. In this regard,  $|E^*|$  will typically be used as a modulus parameter indicative of LVE behaviour of HMA materials at different temperatures and loading frequencies.

Depending on how the laboratory test results of  $|E^*|$  of HMA are interpreted, a variety of information may be obtained. It is imperative to investigate ways in which this information can be used in a mechanistic analysis of pavement structures. For example, plots of  $|E^*|$  versus frequency (rate of loading with time) at multiple temperatures may be shifted to the reduced frequency and aligned to form a single curve known as a master curve. The master curve then becomes a representation of the HMA behaviour at a given reference temperature for a range of frequencies. The HMA dependency on temperature and loading time, as observed from the master curve, is typical of an LVE material. Several researchers have already shown that HMA has viscoelastic behaviour (Goodrich, 1991; SHRP, 1994; Lee and Kim, 1998; Daniel and Kim, 2002). An LVE material exhibits both elastic and viscous behaviour. When an elastic material is deformed by external load into a new equilibrium shape it stores all the energy during the deformation. The material then makes use of this energy to instantaneously return to its original shape upon removal of the external load. On the other hand, a viscous material has no definite shape and its deformation under external load is irreversible because the energy it obtains from external load is continuously dissipated.

If SAPDM is to determine pavement structural responses more accurately in terms of stresses, strains and displacement, it is important that the LVE nature of HMA is incorporated into its analysis engine. It should be stated that although pavements are made of multiple layers of which, each is composed of multi-component discrete elements, the concept of continuum representation is generally accepted. This allows for the use of engineering mechanics principles to express the relationships of stresses, strains and displacements for both linear and LVE materials.

The theory behind dynamic modulus is well documented through several studies (Dougan, *et al.*, 2003; Schwartz, 2005; Witczak, *et al.* 2002; and Yoder and Witczak, 1975). Test procedure/protocol for dynamic modulus testing of South African (SA) HMA mixes was recently developed whereby the dynamic modulus values are determined over a range of values reflecting actual field loading frequencies and temperatures as recorded in SA (Anochie-Boateng *et al.*, 2010).

Two well known viscoelastic programs developed for pavement engineering applications are VEROAD (Hopman *et al.*, 1997) and KENLAYER (Huang, 2004). VEROAD is an LVE multilayer program that uses Burger's as well as Huet-Sayegh rheological models for the HMA materials and transforms the governing equation from time to frequency domain using Fourier transforms. KENLAYER on the other hand, is based on quasi-elastic solutions by the collocation method (Huang, 2004; Schappery, 1961).

Nilsson *et al.* (2002), showed that the two models can be used to characterize LVE behaviour of HMA materials although there were limitations on the frequency range for which Burger's model was able to fit well the laboratory measured complex modulus. Huet-Sayegh model, however, could adequately fit the laboratory measured complex modulus for all the frequency, temperature and phase angle values.

In preparation for future update of SAPDM, this paper demonstrates the use of Burger's and Huet-Sayegh rheological models to characterize LVE behaviour of HMA material at different temperatures and loading frequencies. Further, the paper presents some mathematical formulation that provides guidelines to analyze a multilayered pavement system consisting of one or more layers of LVE materials. The Burger's and Huet-Sayegh models are implemented and incorporated into the analysis algorithm.

A third model, which is an extension of Huet-Sayegh model was proposed by Olard and Di Benedetto (2003) and accounts for the 'pseudo' permanent deformation of the asphalt binder and mixture will also be investigated for possible incorporation. The results from these models, in terms of surface deflections, are compared against results from GAMES software (Maina and Matsui, 2004), which is currently used as the analysis engine for SAPDM.

## 2. VISCO-ELASTIC CONSTITUTIVE MODELING

Constitutive equations are used to mathematically describe the relationship among responses based on a particular behaviour in a continuum mechanics. In an LVE material, the stress is linearly related to the strain history. The strain arising from any increment of the stress will add to the strain resulting from the stresses previously created in the body (Casula and Carcione, 1992).

### 2.1. Dynamic loading test

Stresses in elastic bodies are considered independent of the material constants but deflections are functions of the material constants and will be time dependent. Further, creep test (measure of time dependent strain) and stress relaxation (monitoring time dependent stress resulting from a steady strain) are convenient for studying material response over a longer period of time from minutes to days. But for shorter times, dynamic loading tests (sinusoidal stress-strain loading) are well suited. When an LVE material is subjected to sinusoidal stress, a steady state will eventually be reached resulting in sinusoidal strain having the same angular frequency but retarded in phase by an angle  $\theta$  as shown in Figure 1. For LVE materials, the stress-strain relationship under a continuous sinusoidal loading is defined by a complex number called the complex modulus  $E^*$  (ASTM D 3497, 2003; NCHRP 1-37A, 2004; AASHTO TP 62, 2009). The complex modulus has real and imaginary parts that define the elastic and viscous behaviour of LVE materials. The absolute value of the complex modulus is defined as the material's dynamic modulus  $|E^*|$ .

### 2.1.1 Basic equations

For one-dimensional case of a sinusoidal loading, the applied stress and the corresponding strain can be expressed in a complex form by Equations 1a and 1b, respectively.

$$\sigma^* = \sigma_0 e^{i\omega t} \quad (\text{Eq. 1a})$$

$$\varepsilon^* = \varepsilon_0 e^{i(\omega t - \theta)} \quad (\text{Eq. 1b})$$

where  $\sigma$  is the applied stress,  $\sigma_0$  is the stress amplitude;  $\varepsilon$  is the strain response,  $\varepsilon_0$  is the strain amplitude;  $\omega$  is angular frequency, which is related to frequency by  $\omega = 2\pi f$ ;  $f = 1/T$ ;  $t$  is time, and  $T$  is period;  $\theta$  is the phase angle related to the time the strain lags behind the stress. Phase angle is an indicator of the viscous (or elastic) properties of the viscoelastic material. For a pure elastic material,  $\theta = 0^\circ$ , and for a pure viscous material,  $\theta = 90^\circ$ . Mathematically,  $|E^*|$  is defined as the maximum (peak) dynamic stress divided by the recoverable maximum (peak) axial strain.

From Equations 1a and 1b the complex modulus,  $E^*(i\omega)$ , is defined as the complex quantity in Equation 2.

$$E^*(i\omega) = \frac{\sigma^*}{\varepsilon^*} = \frac{\sigma_0}{\varepsilon_0} e^{i\theta} = E' + iE'' \quad (\text{Eq. 2})$$

The real part of the complex modulus is the storage modulus ( $E'$ ) and the imaginary part is the loss modulus ( $E''$ ). The dynamic modulus  $|E^*|$  is the absolute value of the complex modulus, which is defined mathematically in Equation 3.

$$|E^*| = \frac{\sigma_0}{\varepsilon_0} \quad (\text{Eq. 3})$$

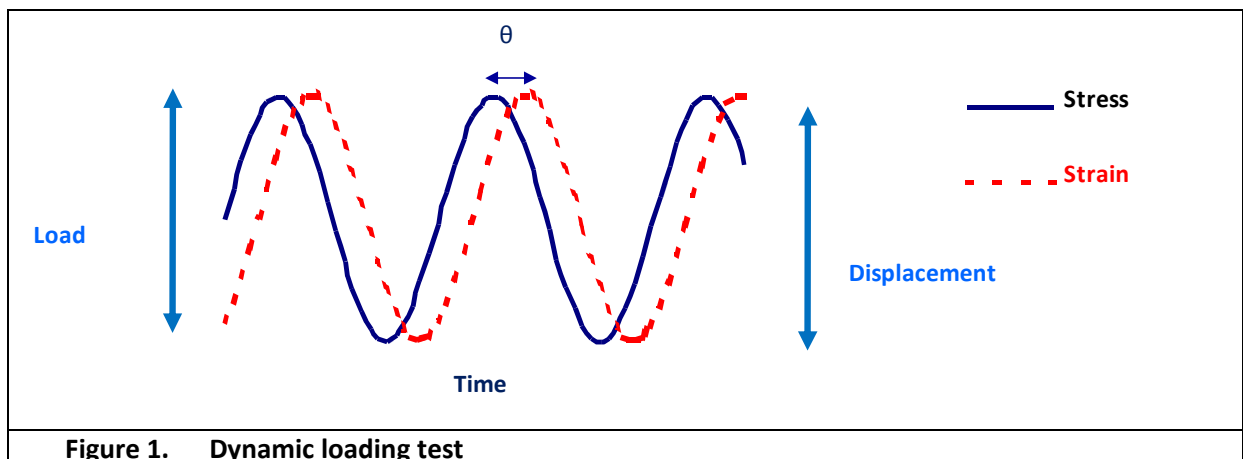


Figure 1. Dynamic loading test

### 2.2. Mathematical models for linear viscoelastic (LVE) response

Another way of describing LVE behaviour of materials is by a discrete combination of linear elastic spring and linear viscous dash-pot elements either in series or parallel (Huang, 2004).

Models built in this manner are known as rheological models or mechanical models. According to Nilsson *et al.* (2002), generalized model and the Huet-Sayegh model have proved to be the most suitable models available for characterizing the mechanical behaviour of LVE materials over a wide range of frequencies and temperature.

A simple case of the generalized model is the Burger's model shown in Figure 2 (Xu and Solaimanian, 2009), which is represented by the arrangement of one Kelvin element (Delayed Elastic) and one Maxwell element (Elastic and Viscous) connected in series. The Kelvin model is used to represent the delayed elastic response ( $\epsilon_{de}$ ), while the elastic spring in the Maxwell model represents the instantaneous elastic response ( $\epsilon_{ie}$ ) and the dash-pot represents the creep behaviour ( $\epsilon_{cp}$ ) of the visco-elastic material. Further, the Huet-Sayegh model shown in Figure 3 (Xu and Solaimanian, 2009) has two parallel branches. One branch has two biparabolic dashpots,  $k$  and  $h$  and a spring  $E_\infty - E_0$  in series, where  $E_\infty$  represents purely elastic modulus,  $E_0$  is the long term behaviour of the materials. The second branch consists of a single spring,  $E_0$ .

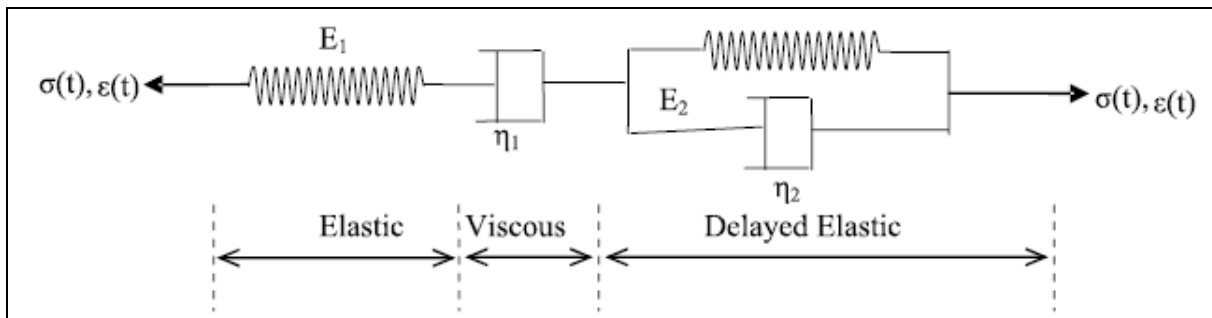


Figure 2. Burger's model (from Xu and Solaimanian, 2009)

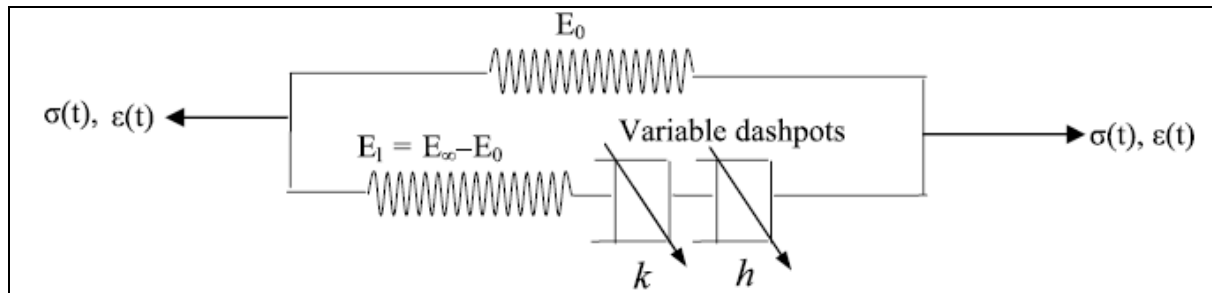


Figure 3. Huet-Sayegh Model (from Xu and Solaimanian, 2009)

### 2.2.1 Burger's model

As an example, derivation of the complex modulus associated with Burger's model will be shown next. Here, the time-dependent solutions in an LVE material may be obtained using the correspondence principle.

Total strain in the Burger's model may be written as:

$$\epsilon = \epsilon_{de} + \epsilon_{ie} + \epsilon_{cp} \quad (\text{Eq. 4.1})$$

Further, stress-strain relationship may be written as:

$$\sigma = E_1 \epsilon_{ie} \quad \sigma = \eta_1 \frac{\partial}{\partial t} \epsilon_{cp} \quad \sigma = E_2 \epsilon_{de} + \eta_2 \frac{\partial}{\partial t} \epsilon_{de} \quad (\text{Eq. 4.2})$$

Substituting Equation 4.2 into Equation 4.1 and rearrange, yields:

$$\left( \frac{\partial^2}{\partial t^2} + \frac{E_1\eta_1 + E_2\eta_1 + E_1\eta_2}{\eta_1\eta_2} \frac{\partial}{\partial t} + \frac{E_1E_2}{\eta_1\eta_2} \right) \sigma = \left( E_1 \frac{\partial^2}{\partial t^2} + \frac{E_1E_2}{\eta_2} \frac{\partial}{\partial t} \right) \varepsilon \quad (\text{Eq. 5})$$

Equation 5 may be written in a simplified general form as:

$$(\alpha_1 D^2 + \alpha_2 D + \alpha_3) \sigma = (\alpha_4 D^2 + \alpha_5 D + \alpha_6) \varepsilon \quad (\text{Eq. 6})$$

Writing Equation 6 as a function of the differential operator  $D = d/dt$ , yields

$$\sigma(t) = E(D) \varepsilon(t) \quad (\text{Eq. 7})$$

Giving the complex modulus for the Burger's model ( $E(D)$ ) as:

$$E(D) = \frac{\alpha_4 D^2 + \alpha_5 D + \alpha_6}{\alpha_1 D^2 + \alpha_2 D + \alpha_3} \quad (\text{Eq. 8})$$

And the coefficients  $\alpha_i$  in Equation 8 are defined as:

$$\alpha_1 = 1, \alpha_2 = \frac{E_1\eta_1 + E_2\eta_1 + E_1\eta_2}{\eta_1\eta_2}, \alpha_3 = \frac{E_1E_2}{\eta_1\eta_2}, \alpha_4 = E_1, \alpha_5 = \frac{E_1E_2}{\eta_2}, \alpha_6 = 0$$

### 2.2.2 Fourier Transform

By using the correspondence principle, it is possible to use the static analysis to obtain solutions in visco-elastic problems. First, the method of Fourier Transform is utilized to remove the time variable from the complex modulus shown in Equation 8. Using Fourier Transform on the differential parameters yields  $i\omega$  from  $D$  and  $-\omega^2$  from  $D^2$  (Kreyszig, 2004). Stress-strain relation in Equation 7 becomes:

$$\sigma(\omega) = E(\omega) \varepsilon(\omega) \quad (\text{Eq. 9})$$

Consequently, Equation 9 for the complex modulus in frequency domain becomes:

$$E(i\omega) = \frac{-\alpha_4 \omega^2 + \alpha_5 i\omega + \alpha_6}{-\alpha_1 \omega^2 + \alpha_2 i\omega + \alpha_3} \quad (\text{Eq. 10})$$

The complex modulus  $E(i\omega)$  no longer contains the differential parameter but rather is now expressed as a function of frequency  $\omega$ .

Complex modulus associated with Huet-Sayegh model may be obtained in the similar manner to become:

$$E(i\omega) = E_0 + \frac{E_\infty - E_0}{1 + \delta(i\omega\tau)^{-k} + (i\omega\tau)^{-h}} \quad (\text{Eq. 11})$$

Where  $E_\infty$  is obtained from the black diagrams (plots of phase angle vs complex modulus) of the mix by extrapolating the curves to zero phase angle. The other parameters  $E_0, k, h, \delta$  are

determined graphically in such a way that the best fit is obtained in the Cole-Cole diagram (plots of loss modulus,  $E''$  vs. storage modulus  $E'$ ) as well as black diagram (Nilsson, *et al.*, 2002).

The temperature dependency of Huet-Sayegh model is governed by parameter,  $\tau$ , which is known as characteristic time and given as a function of temperature as follows:

$$\ln(\tau) = a + bTemp + cTemp^2 \quad (\text{Eq. 12})$$

where:  $a, b, c$  are regression parameters.

In this case, classic solutions derived for a general analysis of a multi-layered elastic systems (Maina and Matsui, 2004) may be utilized to derive solutions for the case visco-elastic materials. This is very important because it shows that the linear visco-elasticity theory is based on linear elasticity theory with the addition of time as a parameter.

### 2.2.3 Determination of model parameters

In the Burger's model, only four parameters have to be determined for each temperature. This can be done by using non-linear least squares regression of a set of measured complex modulus and corresponding phase angles at various frequencies and given temperature. Results from one of the standard SA HMA tested, i.e. continuously graded asphalt mix with 60/70 penetration grade bituminous binder at five test temperatures (-5°C, 5°C, 20°C, 40°C, and 55°C) and six loading frequencies (25, 10, 5, 1, 0.5, and 0.1 Hz) were used in this investigation. The storage modulus ( $E'$ ) and the loss modulus ( $E''$ ) together with the phase angles were determined as shown in Table 1. Further comparisons of the measured versus predicted dynamic modulus is shown in Figure 4.

	$E_1$ (MPa)	$\eta_1$ (MPa·s)	$E_2$ (MPa)	$\eta_2$ (MPa·s)
-5°C	26562	68611	6254	216
5°C	16425	73691	9791	525
20°C	6202	5235	8548	202
40°C	1164	118	3888	20
55°C	154	202	951	8

	$E_1$ (MPa)	$E_\infty$ (MPa)	$\delta$	$k$	$h$	$\tau$
20°C	56	44143	1.60628	0.15813	0.53788	0.014131

However, it is interesting to note that Burger's model did not fare well in Cole-Cole and Black diagrams because of poor predictions of real and imaginary part of the  $E^*$  as well as the phase angles as shown in Figure 4 to Figure 6. On the other hand, Huet-Sayegh model parameters in Table 2 resulted in very good prediction of dynamic modulus, storage modulus, loss modulus

and the corresponding phase as shown in Figure 7 to Figure 9. In these figures, H-S stands for Huet-Sayegh model.

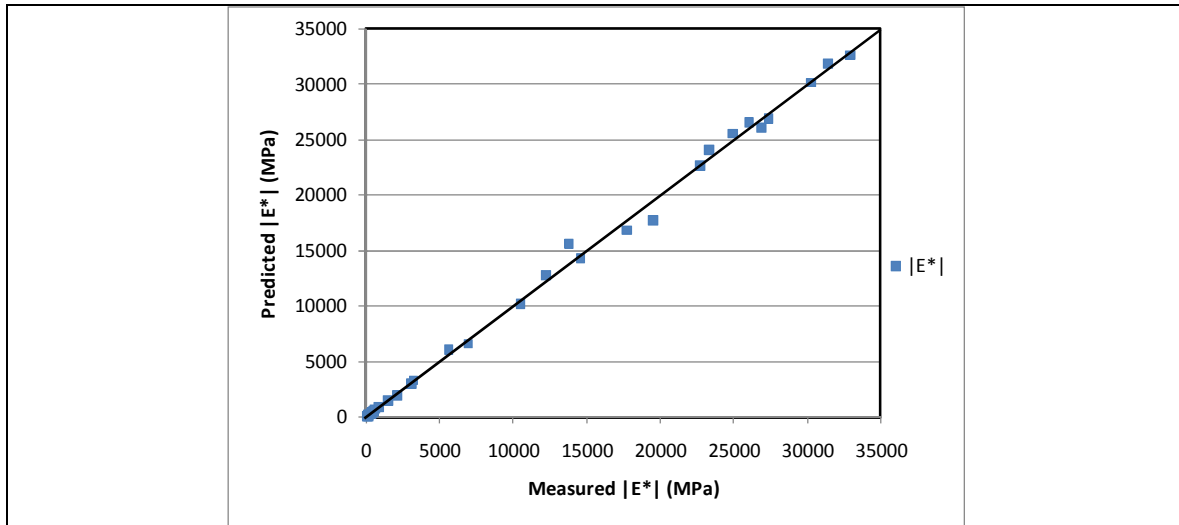


Figure 4. Measured vs. predicted dynamic modulus (Burger's model)

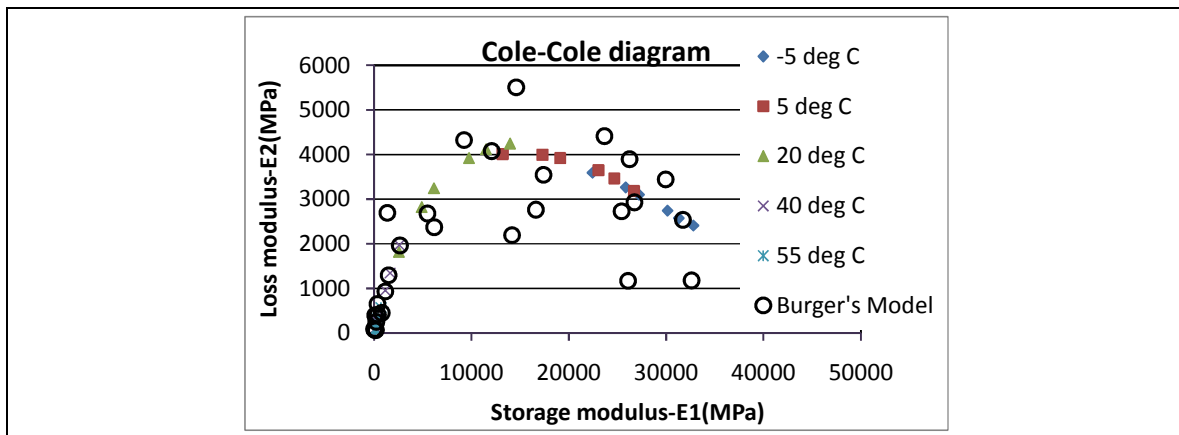


Figure 5. Storage modulus vs. loss modulus (Burger's model)

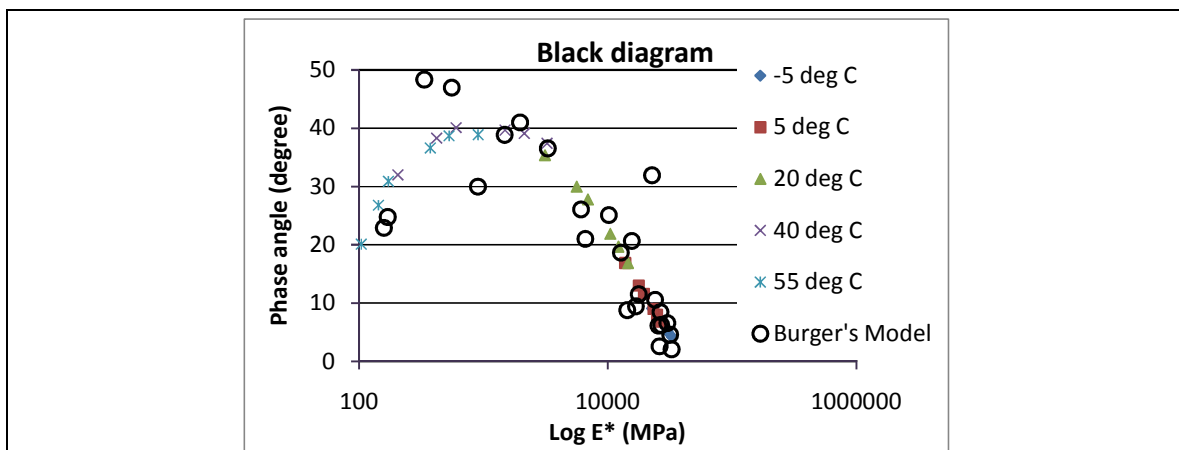


Figure 6. Dynamic modulus vs. phase angle (Burger's model)

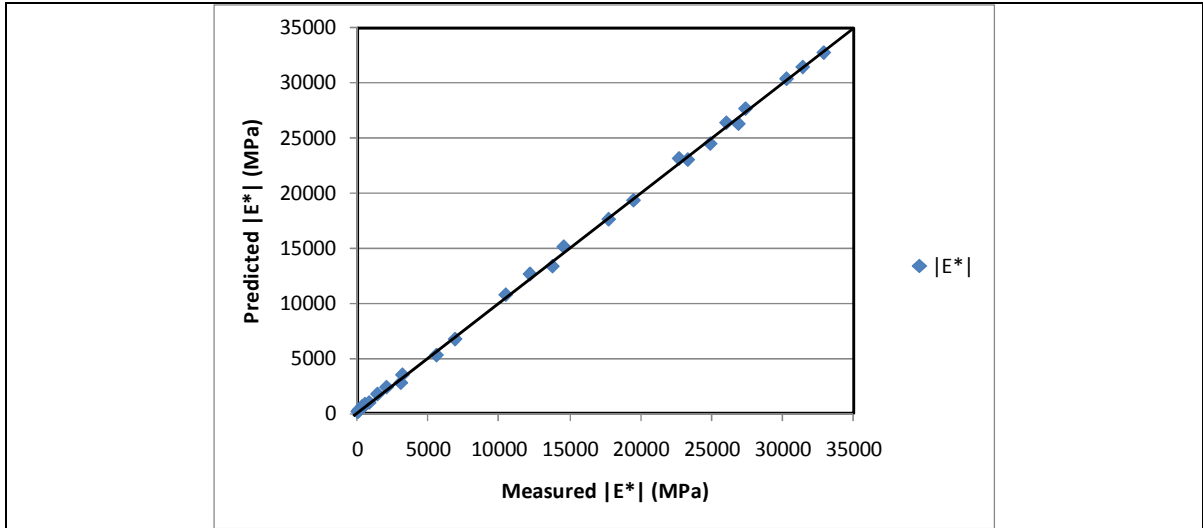


Figure 7. Measured vs. predicted dynamic modulus (Huet-Sayegh model)

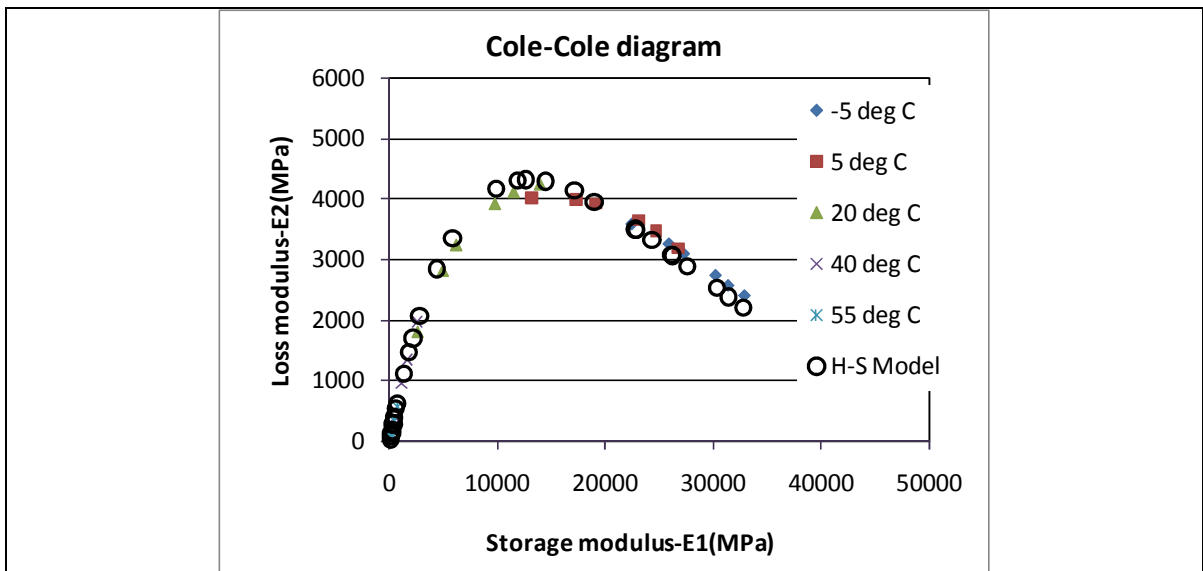


Figure 8. Storage modulus vs. loss modulus ( Huet-Sayegh model )

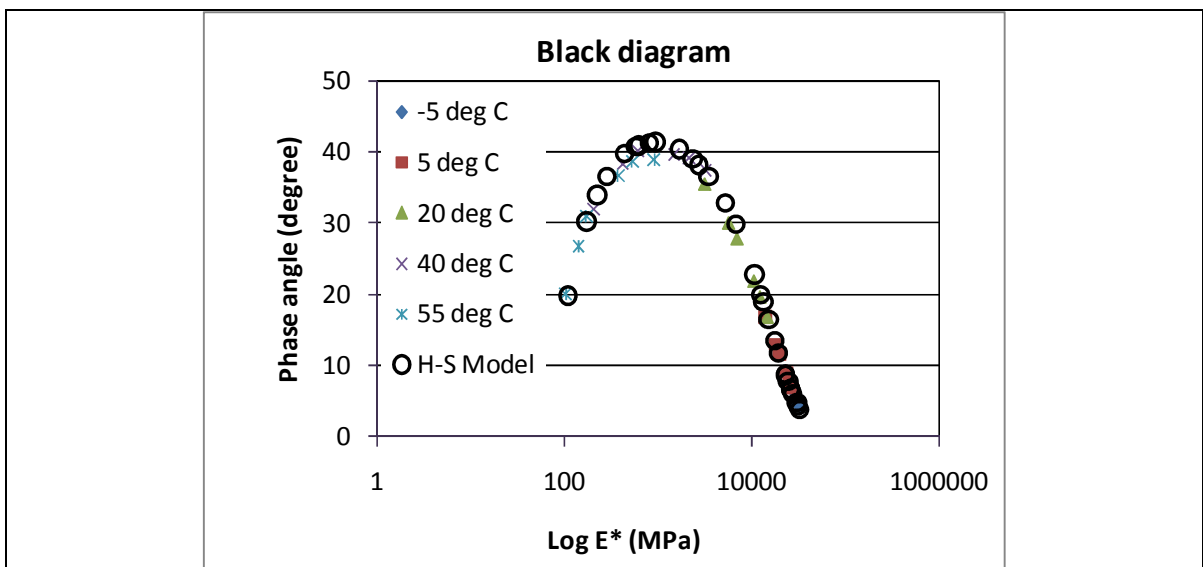


Figure 9. Dynamic modulus vs. phase angle (Huet-Sayegh model)

#### 2.2.4 Mastercurve development using Huet-Sayegh Model

Master curves are commonly employed in the current pavement design methods to characterize the time-temperature dependency of dynamic modulus of HMA materials. The temperature dependency of the  $|E^*|$  is incorporated in the reduced frequency parameter,  $f_r$  in Equation 13. The reduced frequency is defined as the actual loading frequency multiplied by the time-temperature shift factor,  $a(T)$ .

$$\begin{aligned} f_r &= a(T) \times f \\ \log f_r &= \log f + \log a(T) \end{aligned} \quad (\text{Eq. 13})$$

where:

$f$  = frequency, Hz  
 $a(T)$  = shift factor as a function of temperature  
 $T$  = temperature

In the MEPDG, shift factors are expressed as a function of the binder viscosity to allow aging over the life of the pavement to be considered using the Global Aging Model developed by Mirza and Witczak (1995). Equation 14 presents the shift factor relationship used in the MEPDG and followed for the SAPDM.

$$\log a(T) = c (\log \eta - \log \eta_{70\text{RTFO}}) \quad (\text{Eq. 14})$$

where:

$a(T)$  = shift factor as function of temperature and age  
 $\eta$  = viscosity at age and temperature of interest (Pa.s)  
 $\eta_{70\text{RTFO}}$  = viscosity at the reference temperature and RTFO aging  
 $c$  = fitting parameter

Short-term oven aging for 4 hours at 135°C was used to prepare the continuously graded mix. In this condition, the viscosity as a function of temperature was expressed using the ASTM viscosity-temperature relationship given in Equation 15. The NCHRP Project 1-37A (2004) recommends that  $A$  and  $VTS$  parameters could be obtained from several test procedures of the bituminous binder including dynamic shear rheometer, Brookfield viscosity, penetration grade and softening point. Based on availability of viscosity test setup in most laboratories in South Africa, the  $A$  and  $VTS$  parameters used in this study were obtained, exclusively from the Brookfield viscosity tests conducted on the 60/70 penetration grade bituminous binder. An RTFO aging values of  $A$  (= 10.713) and  $VTS$  (= -3.583) obtained from the data analysis were used for the construction of the master curve for the mix.

$$\log \log \eta = A + VTS \log T_R \quad (\text{Eq. 15})$$

where:

$\eta$  = viscosity (Pa.s)  
 $T_R$  = temperature (K)  
 $A$  = regression intercept  
 $VTS$  = regression slope of viscosity temperature susceptibility

By substituting Equation 14 in Equation 13, the shift factors can be obtained as a function of  $A$

and *VTS* parameters with Equation 15. This relationship is used in the MEPDG, and recommended for the construction of dynamic modulus master curves from laboratory test data in SAPDM.

$$\log a(T) = c \left( 10^{A+VTS \log T} - 10^{A+VTS \log(527.67)} \right) \quad (\text{Eq. 16})$$

where:

*c* = fitting parameter

An arbitrary reference temperature adopted for the SAPDM protocol is 20°C instead of 21.1°C used by MEPDG. The reduced frequency as shown in Equation 13 together the Huet-Sayegh model parameters were used to develop master curve for the mix tested and very good results were obtained as shown in Figure 10.

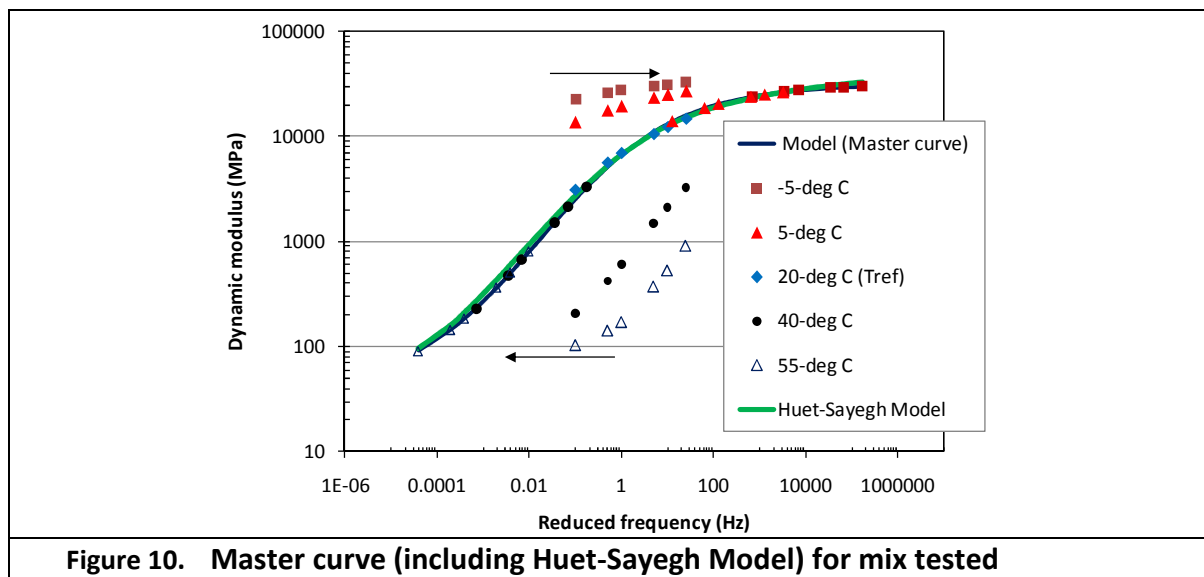


Figure 10. Master curve (including Huet-Sayegh Model) for mix tested

### 3. EQUILIBRIUM EQUATIONS

Having obtained the properties of LVE material using both Burger’s and Huet-Sayegh Model, the next step was to develop numerical algorithm for pavement analysis taking into consideration the LVE properties. By ignoring body forces, equilibrium equations in cylindrical coordinate system are formulated as follows:

$$\frac{\partial \sigma_r}{\partial r} + \frac{\partial \tau_{rz}}{\partial z} + \frac{\sigma_r - \sigma_\theta}{r} = 0 \quad (\text{Eq. 17})$$

$$\frac{\partial \tau_{rz}}{\partial r} + \frac{\partial \sigma_z}{\partial z} + \frac{\tau_{rz}}{r} = 0 \quad (\text{Eq. 18})$$

where  $\sigma_r$  is normal stress in the *r*-axis direction,  $\tau_{rz}$  is shear stress along *r* – *z*-plane,  $\sigma_\theta$  is normal stress in the circumferential ( $\theta$ ) direction and finally,  $\sigma_z$  is normal stress in the *z*-axis direction. Displacement in the *r*-axis direction can be represented as  $u = u(r, z)$  and displacement in the *z*-axis direction can be represented as  $w = w(r, z)$ . For axi-symmetric case, displacement in the circumferential direction is zero, while strains related to the listed stresses

are represented as  $\varepsilon_r, \varepsilon_\theta, \varepsilon_z,$  and  $\gamma_{rz}$ . Similar to the homogeneous case, strain-displacement relationship is as follows:

$$\varepsilon_r = \frac{\partial u}{\partial r}; \varepsilon_\theta = \frac{u}{r}; \varepsilon_z = \frac{\partial w}{\partial z}; \gamma_{rz} = \frac{\partial u}{\partial z} + \frac{\partial w}{\partial r} \quad (\text{Eq. 19})$$

Stress-strain relationship in Equation 7 in cylindrical coordinate system may be written as:

$$\begin{Bmatrix} \sigma_r \\ \sigma_\theta \\ \sigma_z \\ \tau_{zr} \end{Bmatrix} = E(D) \begin{Bmatrix} a+2b & a & a & 0 \\ a & a+2b & a & 0 \\ a & a & a+2b & 0 \\ 0 & 0 & 0 & b \end{Bmatrix} \begin{Bmatrix} \varepsilon_r \\ \varepsilon_\theta \\ \varepsilon_z \\ \gamma_{zr} \end{Bmatrix} \quad (\text{Eq. 20})$$

Where:

$$a = \frac{\nu}{(1+\nu)(1-2\nu)}, b = \frac{1}{(1+\nu)} \text{ and } \nu \text{ is Poisson's ratio, which is assumed to be constant.}$$

Fourier Transform of the stress-strain relationship becomes:

$$\begin{Bmatrix} \bar{\sigma}_r \\ \bar{\sigma}_\theta \\ \bar{\sigma}_z \\ \bar{\tau}_{zr} \end{Bmatrix} = E(i\omega) \begin{Bmatrix} a+2b & a & a & 0 \\ a & a+2b & a & 0 \\ a & a & a+2b & 0 \\ 0 & 0 & 0 & b \end{Bmatrix} \begin{Bmatrix} \bar{\varepsilon}_r \\ \bar{\varepsilon}_\theta \\ \bar{\varepsilon}_z \\ \bar{\gamma}_{zr} \end{Bmatrix} \quad (\text{Eq. 21})$$

Substituting Fourier Transform of Equation 19 into Equation 21, yields:

$$\left\{ (a+2b) \left( \frac{\partial^2}{\partial r^2} + \frac{1}{r} \frac{\partial}{\partial r} - \frac{1}{r^2} \right) + b \frac{\partial^2}{\partial z^2} \right\} \bar{u} + (a+b) \frac{\partial^2 \bar{w}}{\partial r \partial z} = 0 \quad (\text{Eq. 22})$$

$$(a+b) \left( \frac{\partial^2}{\partial r \partial z} + \frac{1}{r} \frac{\partial}{\partial z} \right) \bar{u} + \left\{ b \left( \frac{\partial^2}{\partial r^2} + \frac{1}{r} \frac{\partial}{\partial r} \right) + (a+2b) \frac{\partial^2}{\partial z^2} \right\} \bar{w} = 0 \quad (\text{Eq. 23})$$

Further Hankel Transform of Equations 20 and 22, gives:

$$\left( -(a+2b)\xi^2 + b \frac{\partial^2}{\partial z^2} \right) \tilde{u} - (a+b)\xi \frac{\partial \tilde{w}}{\partial z} = 0 \quad (\text{Eq. 24})$$

$$(a+b)\xi \frac{\partial \tilde{u}}{\partial z} + \left( -b\xi^2 + (a+2b) \frac{\partial^2}{\partial z^2} \right) \tilde{w} = 0 \quad (\text{Eq. 25})$$

Solving for the Hankel and Fourier transformed displacements yields:

$$\tilde{w}(\xi, z, \omega) = Ae^{-\xi z} + Bze^{-\xi z} + Ce^{\xi z} + Dze^{\xi z} \quad (\text{Eq. 26})$$

$$\tilde{u}(\xi, z, \omega) = Ae^{-\xi z} + \frac{-3+4\nu+\xi z}{\xi} Be^{-\xi z} - Ce^{\xi z} + \frac{-3+4\nu-\xi z}{\xi} De^{\xi z} \quad (\text{Eq. 27})$$

Here,  $A, B, C, D$ , which are functions of frequency ( $\omega$ ) and Hankel parameter ( $\xi$ ) are known as constants of integration. Substituting Equations 26 and 27 into Equations 19 and 21 gives expression for the Hankel and Fourier transformed displacements and stresses as follows:

$$\begin{Bmatrix} \tilde{u}(z, \omega, \xi) \\ \tilde{w}(z, \omega, \xi) \\ \tilde{\sigma}_z(z, \omega, \xi) \\ \tilde{\tau}_{rz}(z, \omega, \xi) \end{Bmatrix} = \begin{pmatrix} q_{11} & q_{12} & q_{13} & q_{14} \\ q_{21} & q_{22} & q_{23} & q_{24} \\ q_{31} & q_{32} & q_{33} & q_{34} \\ q_{41} & q_{42} & q_{43} & q_{44} \end{pmatrix} \begin{Bmatrix} A(\omega, \xi) \\ B(\omega, \xi) \\ C(\omega, \xi) \\ D(\omega, \xi) \end{Bmatrix} \quad (\text{Eq. 28})$$

$[q_{ij}]$  is a coefficient matrix for a single layer pavement system, which among others is a function of depth in the pavement layer.

Procedure similar to the one explained in Maina and Matsui (2004) may be followed to extend this method to a multilayered system. In this process the relation between responses at the top and bottom of the layer as well as relation at the interface relating responses at the bottom of one layer to the responses on top of the next are used.

In summary, looking at one layer  $k$ , responses at its surface and at a depth  $h_k$  up to the depth of the layer may be related as:

$$\begin{pmatrix} \tilde{u}^k(0, \omega, \xi) \\ \tilde{w}^k(0, \omega, \xi) \\ \tilde{\sigma}_z^k(0, \omega, \xi) \\ \tilde{\tau}_{rz}^k(0, \omega, \xi) \end{pmatrix} = [q_{ij}^k(0, \omega, \xi)] [q_{ij}^k(h_k, \omega, \xi)]^{-1} \begin{pmatrix} \tilde{u}^k(h_k, \omega, \xi) \\ \tilde{w}^k(h_k, \omega, \xi) \\ \tilde{\sigma}_z^k(h_k, \omega, \xi) \\ \tilde{\tau}_{rz}^k(h_k, \omega, \xi) \end{pmatrix} \quad (\text{Eq. 29})$$

Further, looking at two adjacent layers, the responses at the bottom of layer  $k$  and top of the next layer  $k+1$  can be related as follows:

$$\begin{pmatrix} \tilde{u}^k(h_k, \omega, \xi) \\ \tilde{w}^k(h_k, \omega, \xi) \\ \tilde{\sigma}_z^k(h_k, \omega, \xi) \\ \tilde{\tau}_{rz}^k(h_k, \omega, \xi) \end{pmatrix} = \begin{pmatrix} \tilde{u}^{k+1}(0, \omega, \xi) \\ \tilde{w}^{k+1}(0, \omega, \xi) \\ \tilde{\sigma}_z^{k+1}(0, \omega, \xi) \\ \tilde{\tau}_{rz}^{k+1}(0, \omega, \xi) \end{pmatrix} \quad (\text{Eq. 30})$$

These relationships are then used to transfer the constants of integration for the bottom layer  $k=N$  and relate it to the responses on top of the first layer  $k=1$ . In this case, information on the boundary conditions for the bottom layer when  $z \rightarrow \infty$  dictate that all the responses will be equal to zero. For this to be possible, constants of integrations  $C^{k=N} = D^{k=N} = 0$ .

Boundary conditions considering a uniformly distributed surface ( $z=0$ ) time dependent load,  $P(t)$  over an area of radius,  $a$  are such that:

$$\begin{aligned} r \leq a: \sigma_z &= -p(t) \\ r > a: \sigma_z &= 0 \\ r \geq 0: \tau_{rz} &= 0 \end{aligned} \quad (\text{Eq. 31})$$

Here:  $p(t) = P(t)/\pi a^2$  and  $t$  is the duration at which the load acts on the pavement surface.

Fourier Transform followed by Hankel transform considering boundary condition at the surface of the pavement as well as the time dependent uniformly distributed circular load,  $p(t)$ , whose radius is  $a$  would be given as:

$$\begin{cases} \tilde{\sigma}_z(z=0, \xi, \omega) \\ \tilde{\tau}_{rz}(z=0, \xi, \omega) \end{cases} = \begin{cases} -\tilde{p}(\xi, \omega) \\ 0 \end{cases} \quad (\text{Eq. 32})$$

where,

$$\tilde{p}(\xi, \omega) = \int_0^\infty r p(\omega) J_0(\xi r) dr = \frac{p(\omega) a}{\xi} J_1(\xi a) \quad (\text{Eq. 33})$$

This information is then used to determine the other constants of integration ( $A^{k=N} = B^{k=N}$ ) for the bottom layer. With all the coefficients of integration for the bottom layer known, this information may then be used to determine coefficients of integration for any other layer, and hence responses at any point within that layer. Readers who are interested in the details of this procedure are encouraged to read Maina and Matsui (2004).

The solutions are obtained by carrying out inverse Hankel transform followed by inverse Fourier transform.

#### 4. WORKED EXAMPLE

Visco-elastic materials can be characterized under constant static load or harmonic load. In this example a uniformly distributed circular static load (50 kN over an area of radius 0.15 m). The 0.5 sec load pulse shown in Figure 12 was considered to act on the surface of a three-layer pavement structure shown in Figure 11.

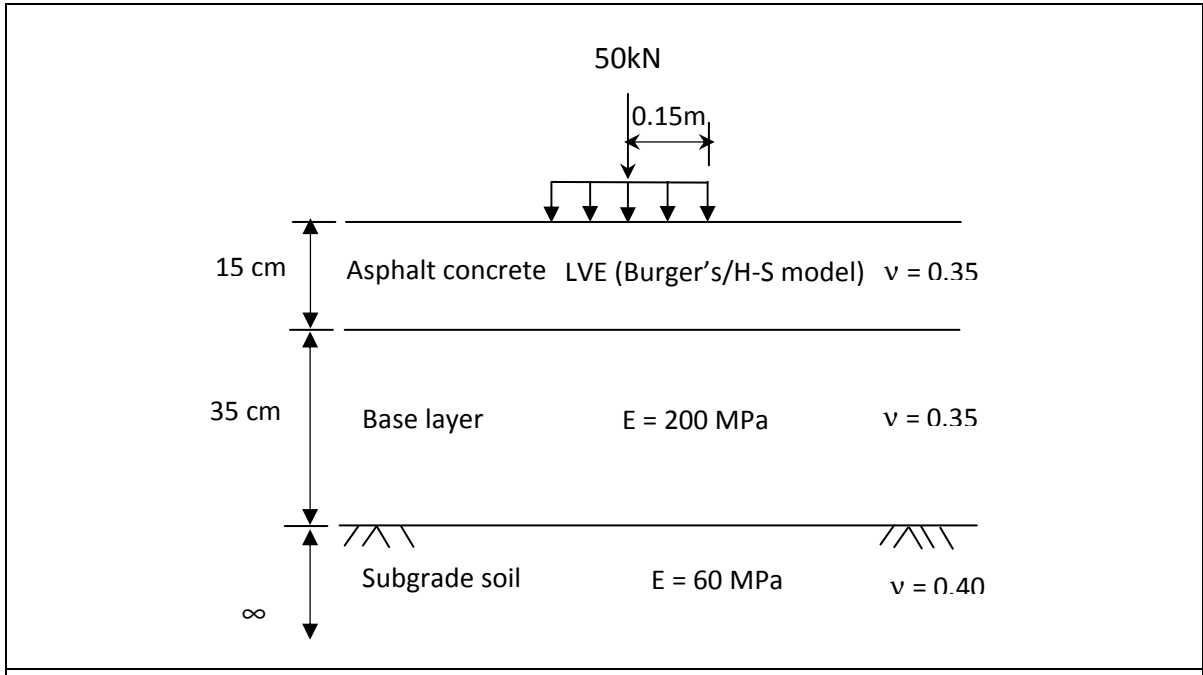


Figure 11. Pavement structure

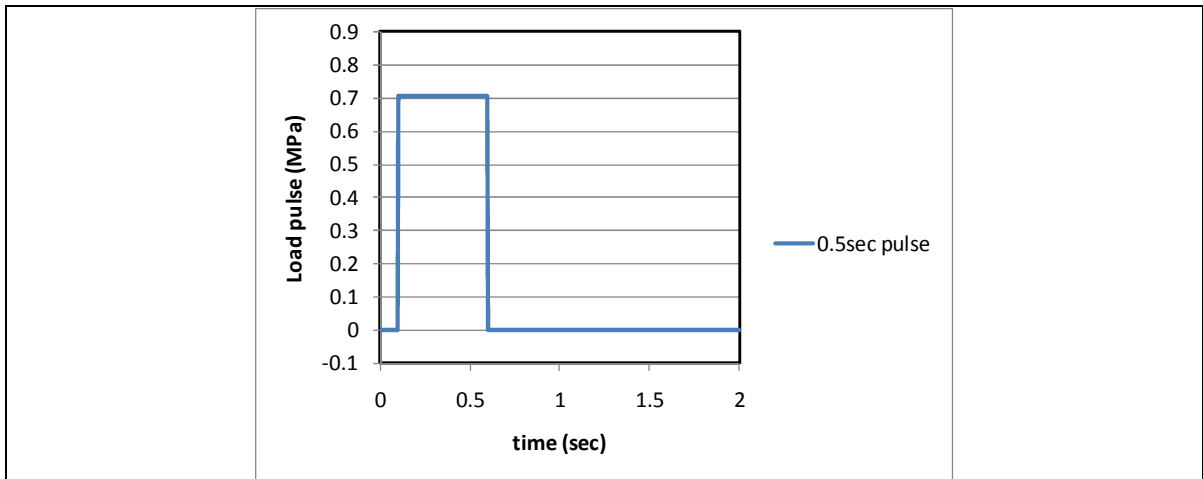


Figure 12. Load pulse (0.5sec) acting on pavement surface

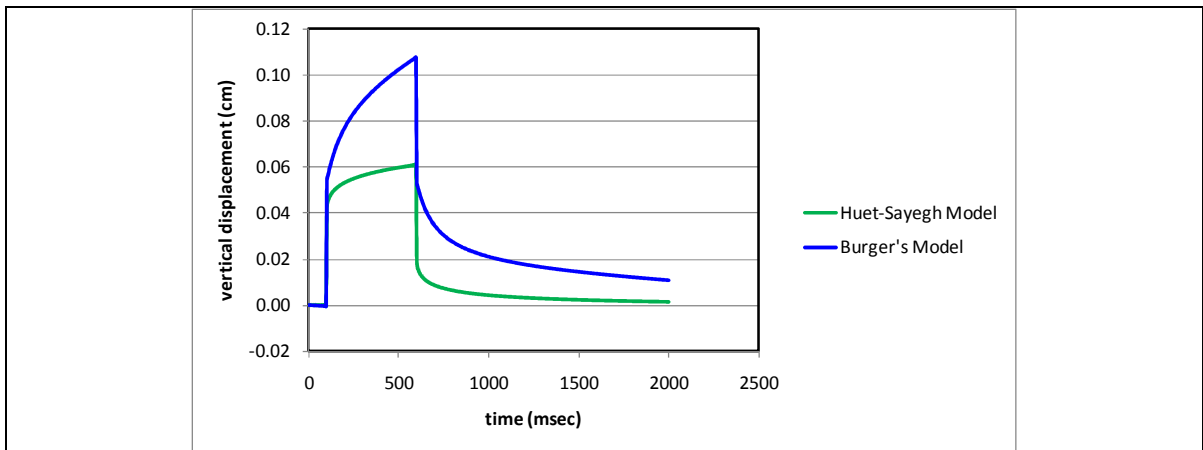


Figure 13. Load pulse (0.5sec) acting on pavement surface

Figure 13 is an example of the preliminary study on the difference of responses that may be obtained by using the two rheological models. Apart from their differences in the prediction of real and imaginary parts of the measured complex modulus as well the corresponding phase angles, the use of Burger's model appear to result in higher responses as compared to when the HMA layer is characterized by Huet-Sayegh model. The amount of instantaneous displacement for the two models appears to be close, but the creep is higher for the burger's model than for the Huet-Sayegh model. Although it is still in early stages of development, similar trend was reported by Sybiliski *et al.* (2004) in their study of polish pavements using veroad software.

## 5. CONCLUSIONS AND RECOMMENDATIONS

This study has been successful in the following areas:

1. Introduction of rheological model for multilayer pavement engineering application using Fourier transform
2. Determination of parameters for Burger's and Huet-Sayegh rheological models for a standard SA asphalt mix, i.e., medium-continuous asphalt mix with 60/70 penetration-grade bituminous binder).
3. Successful representation of Cole-Cole and Black diagrams for both Burger's model and Huet-Sayegh model. However, it appears that Huet-Sayegh model describes better the material properties for the test temperature and frequencies.
4. Mathematical formulation for analysis of pavement structure comprising of LVE layer was implemented.
5. Simple worked example has shown that the two models result in different responses (in this case vertical displacements). Further work is required to validate results presented in this paper before a general conclusion can be drawn.

## ACKNOWLEDGEMENT

Authors would like to acknowledge the assistance from Julius Komba, a candidate researcher at the CSIR Built Environment, for the initial work in the preparation of the standard plots on the material tested.

## REFERENCES

ASTM D3497, 2003. **Standard Test Method for Dynamic Modulus of Asphalt Mixes.**

AASHTO TP 62-07, 2009. **Determining Dynamic Modulus of Hot Mix Asphalt (HMA).** American Association of State Highway and Transportation Officials (AASHTO).

Anochie-Boateng, J., Denneman, E., O'Connell, J. and Ventura, D., 2010. **Hot-mix asphalt testing for the South African pavement design method.** Proceedings of 29th Southern Africa

## 10<sup>th</sup> CONFERENCE ON ASPHALT PAVEMENTS FOR SOUTHERN AFRICA

transportation conference, Pretoria, pp 111-128.

Casula, G and Carcione, J.M. 1992., **Generalized Mechanical Model Analogies of Linear Viscoelastic Behaviour**. Bollettino di geofisica teorica ed applicata, Vol. xxxiv n. 136.

Daniel, J. S. & Kim, Y. R., 2002. *“Development of a Simplified Fatigue Test and Analysis Procedure using a Viscoelastic, Continuum Damage Model”*. **Journal of the Association of Asphalt Paving Technologists**, AAPT.

Dougan, C.E., Stephens, J.E., Mahoney, J. and Hansen, G., 2003. **E\* - Dynamic Modulus. Test Protocol – Problems and Solutions**. Report No. CT-SPR-0003084-F-03-3. University of Connecticut, Storrs, CT.

Goodrich, J. L., 1991. **Asphaltic Binder Rheology, Asphalt Concrete Rheology and Asphalt Concrete Mix Properties**. Journal of the Association of Asphalt Paving Technologists, AAPT, v. 60, p. 80-120.

Hopman P., Nilsson R., Pronk A., 1997. **Theory, validation and application of the visco-elastic multilayer program VEROAD**. 8<sup>th</sup> International Conference on Asphalt Pavements (ICAP), Seattle, USA.

Huang, Y. H. 2004. **Pavement Design and Analysis**. 2<sup>nd</sup> Edition. Prentice Hall.

Kreyszig, E. 1998. **Advanced Engineering Mathematics**. 8<sup>th</sup> Edition. Wiley.

Lee, H. J. and Kim, Y. R., 1998. **Viscoelastic Constitutive Model for Asphalt Concrete under Cyclic Loading**. Journal of Engineering Mechanics, v. 124, n° 1, p. 32-40.

Maina, J. W. and K. Matsui., 2004. **Developing Software for Elastic Analysis of Pavement Structure Responses to Vertical and Horizontal Surface Loadings**. Transportation Research Records, No. 1896, pp. 107-118.

Mirza, M. W., and Witczak, M.W. 1995. **Development of a Global Aging System for Short and Long Term Aging of Asphalt Cements**. Journal of the Association of Asphalt Paving Technologists, Volume 64, Portland, Oregon, USA.

NCHRP 1-37A., 2004. **Development of the 2002 Guide for the Design of New and Rehabilitated Pavement Structures: Phase II**.

Nilson, R. N., Hopman, P. C., and Isacsson, U., 2002. **Influence of Different Rheological Models on Predicted Pavement Responses in Flexible Pavements**. International Journal of Road Materials and Pavement Design (RMPD), Vol. 3, Issue 2.

Olard, F. and Di Benedetto, H., 2003. **General "2S2P1D" model and relation between the linear viscoelastic behaviors of bituminous binders and mixes**, International Journal of Road Materials and Pavement Design (RMPD), vol. 4, n° 2, pp. 185-224.

SHRP., 1994. **SHRP-A-415 – Permanent Deformation Response of Asphalt Aggregate Mixes”**. Strategic Highway Research Program, Washington, D.C., Estados Unidos.

## 10<sup>th</sup> CONFERENCE ON ASPHALT PAVEMENTS FOR SOUTHERN AFRICA

Schapery, R. A., 1961. **A simple collocation method for fitting viscoelastic models to experimental data.** GALCIT SM 61-23A, California Institute of Technology, Pasadena, CA.

Schwartz, C.W., 2005. **Evaluation of the Witczak Dynamic Modulus Prediction Model.** 84th Annual Meeting of the Transportation Research Board, Paper No. 05-2112, Washington D.C., 2005.

Sybilski, D., Mularzuk, R., and Bankowski, W. 2004. **Comparison between Typical Pavement Structure in Accordance with Polish Design Guide and Innovation Pavement Structure with use of Veroad Software.** 2<sup>nd</sup> International Congress SIIV, Florence, Italy.

Theyse H. L., de Beer M and Rust F. C. 1996. **Overview of the South African Mechanistic Pavement Design Method.** Transportation Research Record 1539. Transportation Research Board, Washington D.C.

Witczak, M.W., Kaloush, K., Pellinen, T., El-Basyouny, M., and Von Quintus, H. 2002. **Simple Performance Test for Superpave Mix Design.** NCHRP Report 465, Transportation Research Board, Washington, D.C.

Xu, Q. and Solaimanian, M. 2009. **Modelling linear viscoelastic properties of asphalt concrete by the Huet-Sayegh model.** International Journal of Pavement Engineering, 10: 6, 401 — 422

Yoder, E. J., and Witczak, M. W. 1975. **Principles of Pavement Design.** Wiley, New York.